

Solar-, monsoon- and Kuroshio-influenced thermocline depth and sea surface salinity in the southern Okinawa Trough during the past 17,300 years

Libo Wang^{1,2} · Jun Li² · Jingtao Zhao² · Helong Wei² · Bangqi Hu² · Yanguang Dou² · Zhilei Sun² · Liang Zou² · Fenglong Bai²

Received: 6 December 2015 / Accepted: 31 March 2016 / Published online: 7 April 2016
© Springer-Verlag Berlin Heidelberg 2016

Abstract Factors influencing millennial-scale variability in the thermocline depth (vertical mixing) and sea surface salinity (SSS) of the southern Okinawa Trough (OT) during the past 17,300 years were investigated based on foraminifer oxygen isotope records of the surface dweller *Globigerinoides ruber* sensu stricto and the thermocline dweller *Pulleniatina obliquiloculata* in the AMS ¹⁴C dated OKT-3 core. The thermocline depth is influenced by surface thermal buoyancy (heat) flux, in turn controlled by the annual mean insolation at 30°N and the strength of the East Asian winter monsoon (EAWM). Strong insolation and weak EAWM tend to increase buoyancy gain (decrease buoyancy loss), corresponding to shallow thermocline depths, and vice versa. Regional SSS is influenced by the global ice volume, the Kuroshio Current (KC), and vertical mixing. A deep thermocline coincides with a high SSS because strong vertical mixing brings more, saltier subsurface KC water to the surface, and vice versa. Local SSS (excluding the global ice volume effect) became lower in the northern OT than in the southern OT after ~9.2 ka, implying that Changjiang diluted water had stronger influence in the northern sector. SSS show no major changes during the Bølling/Allerød and Younger Dryas events, probably because the KC disturbed the North Atlantic signals. This argues against earlier interpretations of sea surface

temperature records of this core. Wavelet and spectral analyses of the $\Delta\delta^{18}\text{O}_{\text{P-G}}$ ($\delta^{18}\text{O}$ of *P. obliquiloculata* minus *G. ruber* s.s.) and $\delta^{18}\text{O}_{\text{local}}$ records display 1,540-, 1,480-, 1,050-, 860-, 640-, and 630-year periods. These are consistent with published evidence of a pervasive periodicity of 1,500 years in global climate as well as EAWM and KC signatures, and a fundamental solar periodicity of 1,000 years and intermediary derived periodicity of 700 years.

Introduction

The East China Sea (ECS) is a marginal sea in the northwestern Pacific with one of the widest continental shelves in the world. It is bounded by the Chinese continent to the west, the island of Taiwan to the southwest, the Ryukyu Islands to the southeast, Kyushu Island to the northeast and the Korean Peninsula to the north. The continental shelf shallower than 200 m occupies most of the ECS. The Okinawa Trough (OT) is a curved basin behind the Ryukyu Island Arc, and constitutes the southeastern part of the ECS with maximum water depth exceeding 2,000 m (Fig. 1). As a passage between continental China and the northwestern Pacific Ocean, the OT is expected to have recorded paleo-environmental changes rooted in both continental and oceanic influence during the last glacial–postglacial period.

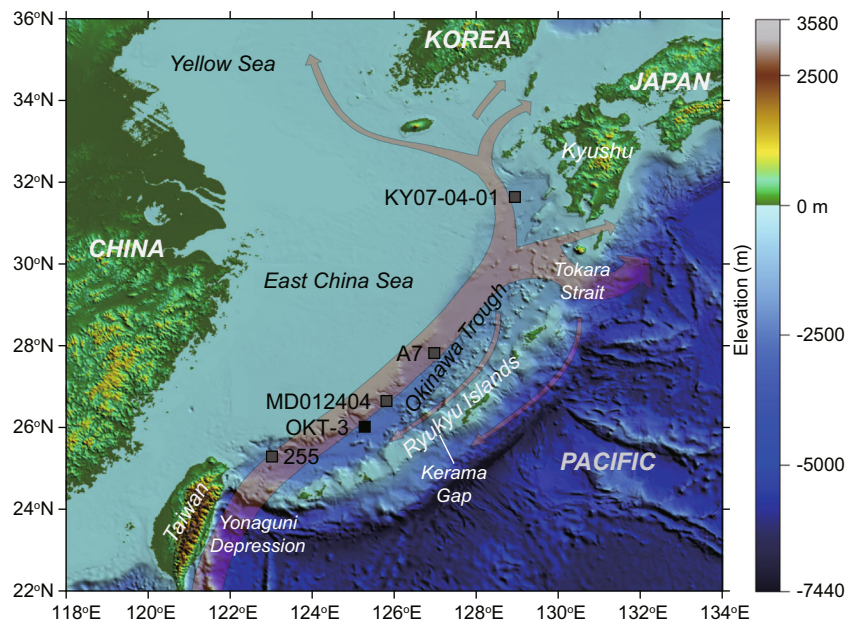
The paleo-environmental evolution of the OT and surrounding areas since the last glacial period has received ever-increasing attention this last decade, based on investigations of multi-proxies such as planktonic foraminifera assemblages and their $\delta^{18}\text{O}$, $\delta^{13}\text{C}$ and Mg/Ca signatures, the U_{37}^K and TEX_{86} temperature proxies, as well as pollen, bulk biogenic and lithogenic characteristics (e.g., Ujiie and Ujiie 1999; Xu and Oda 1999; Jian et al. 2000; Ujiie et al. 2003; Ijiri et al.

✉ Jun Li
junli741001@gmail.com

¹ Key Laboratory of Submarine Geosciences and Prospecting Techniques, Ministry of Education, College of Marine Geosciences, Ocean University of China, Qingdao 266100, China

² Key Laboratory of Marine Hydrocarbon Resource and Environmental Geology, Ministry of Land and Resources, Qingdao Institute of Marine Geology, Qingdao 266071, China

Fig. 1 Locations of core OKT-3 of the present study, and other cores in the Okinawa Trough. Shaded arrows Kuroshio Current and its branches



2005; Kao et al. 2005, 2006a, 2008; Sun et al. 2005; Zhao et al. 2005, 2015; Lin et al. 2006; Xiang et al. 2007; Zhou et al. 2007; Chang et al. 2008, 2009; Yu et al. 2009; Chen et al. 2010; Kubota et al. 2010; Zhang et al. 2010; Xu et al. 2013; Yamamoto et al. 2013; Zheng et al. 2014; Ruan et al. 2015). On glacial–interglacial timescales, surface water transformed from coastal water to open-sea water, sea surface temperature (SST) increased by about 3 °C, and $\delta^{18}\text{O}$ of seawater (an indicator of sea surface salinity, SSS) decreased by more than 1‰ in the OT from the last glacial maximum to the Holocene (Xu and Oda 1999; Ujiie et al. 2003; Ijiri et al. 2005; Sun et al. 2005; Zhao et al. 2005; Yu et al. 2009; Chen et al. 2010; Kubota et al. 2010; Yamamoto et al. 2013; Ruan et al. 2015). Although thermocline depth or mixed layer thickness is also an important parameter of upper water hydrographic conditions, its changes in the OT since the last deglaciation have received insufficient attention. For example, the records of Jian et al. (2000) are limited to the Holocene.

A series of rapid, millennial-scale climate events has marked the last deglaciation, such as the Bølling/Allerød (B/A) warm event and the Younger Dryas (YD) cold event (Bond et al. 1993; Dansgaard et al. 1993; Grootes et al. 1993). Suborbital oscillations of SST and planktonic foraminifera assemblages in the OT were synchronous with these abrupt events, suggesting a teleconnection between the northwestern Pacific and the North Atlantic during the last deglaciation (Ijiri et al. 2005; Sun et al. 2005; Xiang et al. 2007; Yu et al. 2009; Kubota et al. 2010). Millennial-scale climate changes occurred also in the Holocene, such as ice-rafted debris events in the North Atlantic (Bond et al. 1997, 2001), cooling events in the Arabian Sea (Sirocko et al. 1996), and reduced rain fall episodes recorded in the Dongge Cave of SW China (Wang et al. 2005). Several Holocene events identified in the OT are

considered to be the manifestation of the millennial-scale climate cycle (Jian et al. 2000; Xiang et al. 2007; Zheng et al. 2014). It is widely accepted that the dynamic mechanisms of millennial-scale climate changes could be due to reduction or shutdown of the thermohaline circulation (THC) in the North Atlantic via atmospheric teleconnection (Wu et al. 2008). However, SST influenced by the KC in the OT varied asynchronously with epicontinental vegetation of the ECS influenced by atmospheric circulation linked to the northern high-latitude climate, and the terrestrial deglacial warming lagged behind the marine climate changes by 3–4 ka (Xu et al. 2013). SSS oscillations associated with the B/A and YD events are not obvious in the OT (Sun et al. 2005; Chen et al. 2010; Kubota et al. 2010). The millennial-scale climate changes in the OT may be associated with not only North Atlantic but also tropical (Sun et al. 2005) and Antarctic-like influences (Chen et al. 2010). Evidently, more high-resolution oceanic records are necessary for better understanding the dynamic mechanisms of the millennial-scale climate changes in the OT, and the linkage between the northwestern Pacific and the global climate system.

Here, the AMS ^{14}C dated core OKT-3 from the southern OT is selected to evaluate factors governing millennial-scale changes in the thermocline depth (vertical mixing) and SSS. SSTs of this core have been reconstructed by Zhao et al. (2015) using three independent proxies (foraminiferal Mg/Ca ratios, TEX_{86} , and U_{37}^{K}), which were concurrent with the spread of North Atlantic cold signals during the Heinrich Stadial 1 and YD periods, but corresponded to the timing of the Antarctic Cold Reversal during the B/A period. In the present study, two high-resolution planktonic foraminifera $\delta^{18}\text{O}$ records of the surface layer dweller *Globigerinoides ruber sensu stricto* (*G. ruber* s.s.) and the thermocline dweller

Pulleniatina obliquiloculata (*P. obliquiloculata*) served to investigate the thermocline depth. SSS was evaluated by calculating $\delta^{18}\text{O}$ of seawater based on the *G. ruber* s.s. $\delta^{18}\text{O}$ and Mg/Ca-SST data. Moreover, wavelet and spectral analyses enabled searching for suspected evidence of periodicity in the thermocline depth and SSS data.

Oceanographic setting

As an important oceanographic phenomenon in the OT, the KC originates from the northward branch of the bifurcated North Equatorial Current off the Philippine coast, enters the OT in the ECS through the Yonaguni Depression, flows north-eastward along the shelf slope of the ECS near the 200 m isobath, and then reenters the open Pacific through the Tokara Strait (Fig. 1). Its width along the entire stream is ~210 km on average (Liu and Gan 2012), the maximum influence depth reaches ~800 m (Oka and Kawabe 2003; Andres et al. 2008, 2015), and the long-term mean relative transport through the PN section (124.5°E, 30°N to 128.2°E, 27.5°N) is 25.8 Sv for the period 1973 to 2000 (Ichikawa and Beardsley 2002). The volume transport and axis location of the KC vary seasonally due to the influence of the East Asian monsoon (Kagimoto and Yamagata 1997; Ichikawa and Beardsley 2002; Qu and Lukas 2003; Liu and Gan 2012).

Mean SST and SSS in the ECS are characterized by both spatial and seasonal variability (Fig. 2a–d). SST and SSS increase generally from the northwest to southeast. Fresher summer surface water in the northwestern ECS reflects stronger discharge of the Changjiang River, forming Changjiang diluted water (CDW) by mixing with saline ambient water. Core OKT-3 of this study was collected along the main axis of the KC. As shown in the temperature and salinity profiles at the core site (Fig. 2e, f), the summer and winter mean temperatures decrease downward. The summer and winter mean salinities peak at 150–200 m water depth, reflecting the influence of the KC. In summer, the thermocline depth is about 5–20 m on the shelf and about 20–50 m along the Kuroshio; in winter, the thermocline depth is about 15–50 m on the shelf but up to 200 m along the Kuroshio (Hao et al. 2012).

Materials and methods

Piston core OKT-3 (26.018°N, 125.282°E; core length of 5.13 m; water depth of 1,792 m) was retrieved from the southern OT in 2012 (Fig. 1). Sediments in the core consist of homogeneous brown-grey clay and silt, without any obvious turbidites or tephra layers.

An age model for the core was reported by Zhao et al. (2015). For accelerator mass spectrometry radiocarbon (AMS ^{14}C) dating, mono-specific planktonic foraminiferal

shells of *Neogloboquadrina dutertrei* (>150 μm) were picked from six horizons and analyzed at Beta Analytic Inc., USA. All measured AMS ^{14}C ages were calibrated to calendar ages using CALIB 7.1 software (Stuiver and Reimer 1993), the MARINE13 calibration curve (Reimer et al. 2013), and a regional ^{14}C reservoir age of 29 ± 18 years (Delta R, local deviation from the global mean reservoir correction of 400 years) determined from mollusk shells in the western subtropical Pacific (Yoneda et al. 2007). The age model was constructed by linear interpolation between age control points (Fig. 3). Age at the top of the core was assumed to be 0 ka by referring to nearby cores; age at the bottom was estimated to be 17.3 ka by linear extrapolation.

Samples were taken from the core at 4 cm intervals, yielding 128 samples with an average sample resolution of ~135 years. The foraminifers *G. ruber* s.s. and *P. obliquiloculata* were picked from the 250 to 350 μm size fraction of each sample for oxygen isotope analyses. The shells were rinsed with methanol, sonicated for ~10 s, and then oven dried at 40 °C. Analyses were by means of an Isoprime isotope ratio mass spectrometer at the State Key Laboratory of Marine Geology at Tongji University. All $\delta^{18}\text{O}$ values were calculated relative to Vienna Pee Dee Belemnite (VPDB) using the NBS19 standard, with an analytical precision better than $\pm 0.06\text{‰}$. Note that the $\delta^{18}\text{O}$ data of *G. ruber* s.s. have been published by Zhao et al. (2015), but essentially without interpretation or discussion.

G. ruber s.s. is considered to be a reliable tropical or subtropical sea surface hydrographic indicator, as its habitat depth is confined to the upper 30 m of the mixed layer (Ravelo and Fairbanks 1992; Wang 2000). *P. obliquiloculata* is known as a thermocline dweller at the top of the thermocline or at the bottom of the mixed layer in the western Pacific (Pflaumann and Jian 1999). Therefore, stable isotopes of *G. ruber* s.s. and *P. obliquiloculata* reflect seawater hydrographic conditions at the sea surface and at the top of the thermocline layer (or bottom of the mixed layer), respectively. According to sediment trap data from the OT, fluxes of *G. ruber* and *P. obliquiloculata* occur throughout the year (Yamasaki and Oda 2003; Xu et al. 2005). The flux of *P. obliquiloculata* has no obvious seasonal changes (Xu et al. 2005). Although the flux of *G. ruber* is only marginally lower in winter than in other seasons (Xu et al. 2005), this winter effect cannot be neglected.

Results

Foraminiferal oxygen isotope

The $\delta^{18}\text{O}$ values of *G. ruber* s.s. are lighter than those of *P. obliquiloculata* (Fig. 4a). The former vary from -0.5 to -3‰ , the latter from 0.5 to -1.5‰ . The $\delta^{18}\text{O}$ curves

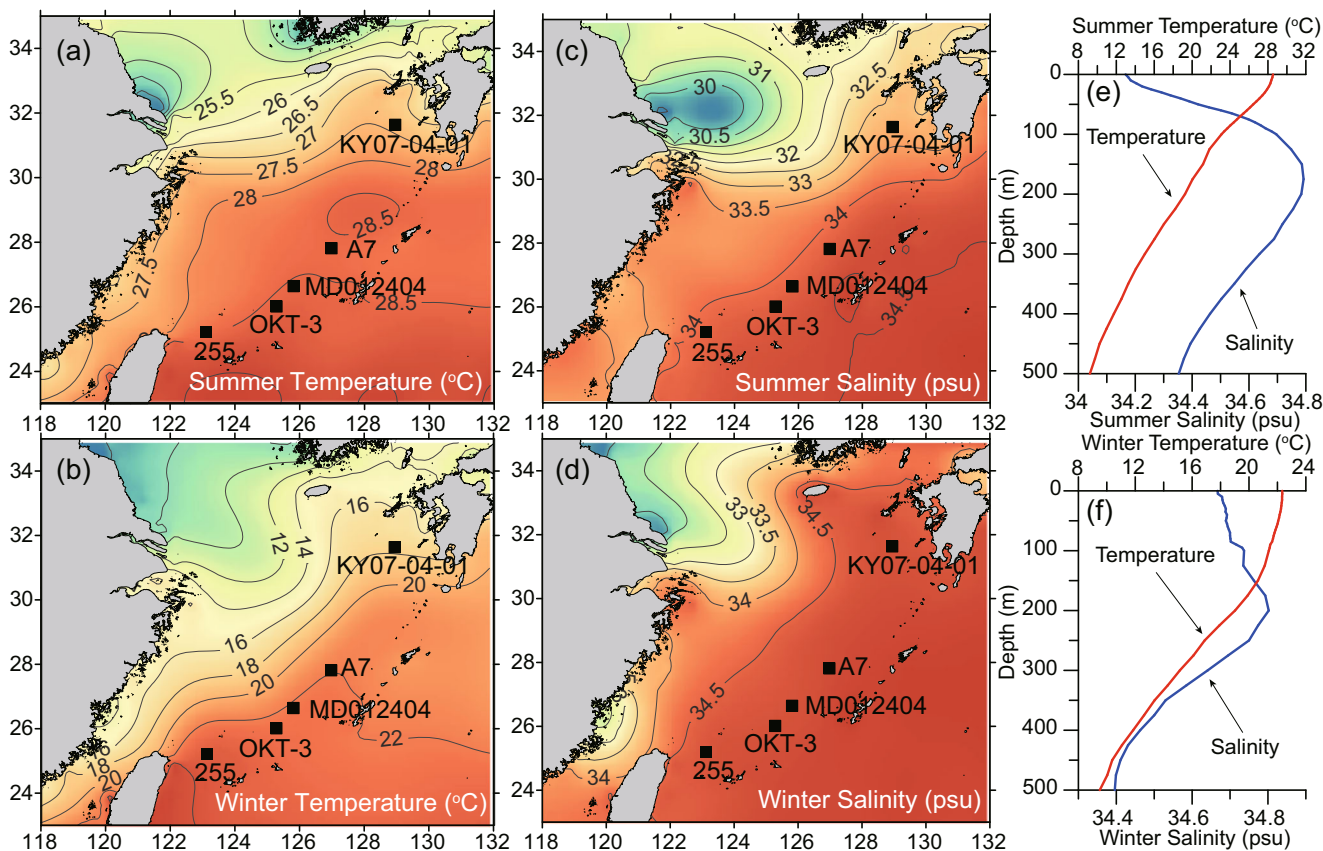


Fig. 2 Seasonal mean sea surface temperature (SST) and salinity (SSS) in the Okinawa Trough and vicinity, and corresponding profiles at the OKT-3 core site: **a** summer SST, **b** winter SST, **c** summer SSS, **d** winter

SSS, **e** temperature and salinity profiles in summer and **f** in winter. Data source: WOA13 (Locamini et al. 2013; Zweng et al. 2013)

both display long-term lightening trends in the past 17, 300 years.

Upper water thermocline hydrography

Previous studies have suggested that the $\delta^{18}\text{O}$ difference between the thermocline dwelling *P. obliquiloculata* and surface dwelling *G. ruber* could indicate the thermocline depth in

tropical and subtropical seas (Jian et al. 2000; Tian et al. 2005), whereby a large difference usually indicates a shallow thermocline and weak upper water mixing, the reverse being the case for a small difference. In the present study, variations of $\Delta\delta^{18}\text{O}_{P-G}$ ($\delta^{18}\text{O}$ of *P. obliquiloculata* minus *G. ruber* s.s.) indicate that the thermocline depth was deep at ~16.5–14.5 ka but shallow at ~14–8 ka. It then increased slightly at ~7.5–4 ka, and decreased slightly at ~2.5 ka (Fig. 4b).

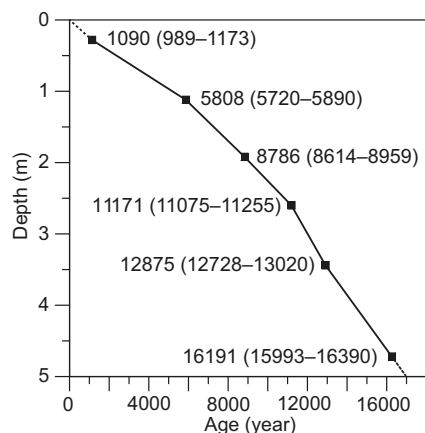


Fig. 3 Age model of core OKT-3 (calendar ages with 2σ ranges; extracted from Zhao et al. 2015)

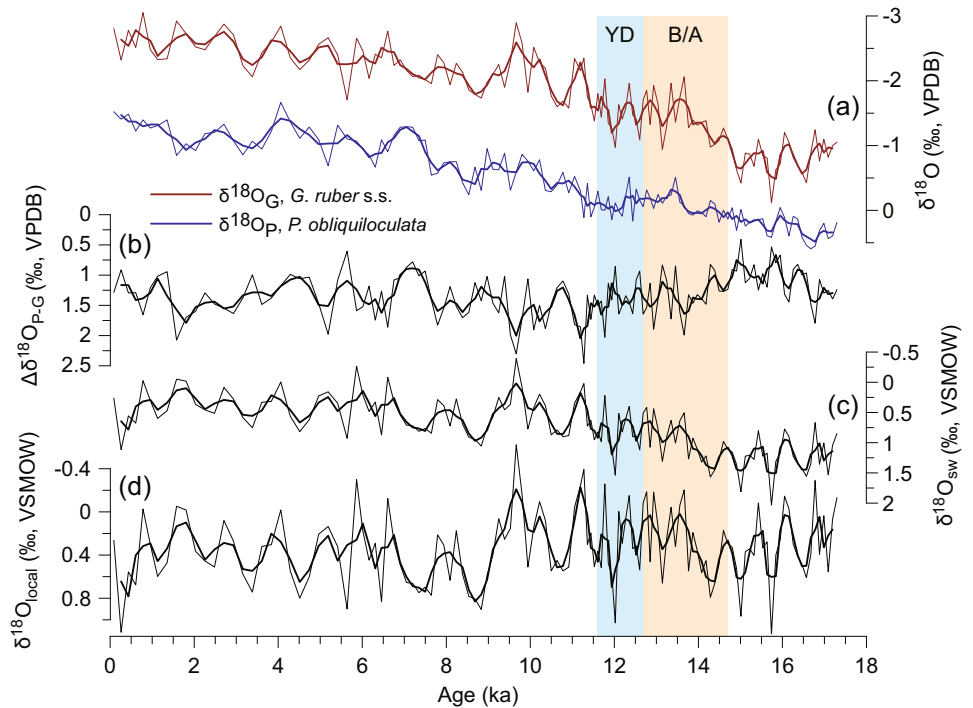
Sea surface water oxygen isotope

The oxygen isotope ratio of foraminiferal calcite ($\delta^{18}\text{O}_c$) depends on the oxygen isotope ratio of ambient seawater ($\delta^{18}\text{O}_{sw}$) in which the foraminifer lives, and seawater temperature that impacts on the oxygen fractionation between the foraminiferal shell and seawater. Due to correlations between $\delta^{18}\text{O}_c$, $\delta^{18}\text{O}_{sw}$ and seawater temperature not having been established for the western Pacific, an empirical equation based on laboratory culturing experiments is used to calculate $\delta^{18}\text{O}_{sw}$ in this study (cf. Bemis et al. 1998):

$$\delta^{18}\text{O}_{sw} = (T - 14.9 + 4.8 * \delta^{18}\text{O}_c) / 4.8 + 0.27$$

where $\delta^{18}\text{O}_c$ is the measured $\delta^{18}\text{O}$ of *G. ruber* s.s., T is the Mg/Ca-based temperature of *G. ruber* s.s. (in the present case,

Fig. 4 Variations of oxygen isotope signatures in core OKT-3 during the past 17,300 years. **a** $\delta^{18}\text{O}_G$ and $\delta^{18}\text{O}_P$, $\delta^{18}\text{O}$ of *G. ruber* s.s. and *P. obliquiloculata* calcite; **b** $\Delta\delta^{18}\text{O}_{P-G}$, $\delta^{18}\text{O}_P$ minus $\delta^{18}\text{O}_G$; **c** $\delta^{18}\text{O}_{sw}$, $\delta^{18}\text{O}$ of seawater; **d** $\delta^{18}\text{O}_{local}$, $\delta^{18}\text{O}$ of seawater with global ice volume effect removed. Shaded bars Younger Dryas cold event (YD) and Bølling/Allerød warm event (B/A)



extracted from Zhao et al. 2015), and 0.27 is the correction from VPDB to VSMOW values. The $\delta^{18}\text{O}_{sw}$ data exhibit a generally lightening trend from 2 to ‰ (VSMOW) between 17.3 and ~9.2 ka, and then fluctuations around 0.4‰ (VSMOW) after ~9.2 ka (Fig. 4c). Even though $\delta^{18}\text{O}_{sw}$ is not a simple paleo-salinity proxy (LeGrande and Schmidt 2011), it still reflects seawater salinity because the two parameters usually have a positive linear relationship. Indeed, the $\delta^{18}\text{O}_{sw}$ data suggest that SSS in the southern OT steadily decreased during the last deglaciation, and became relatively stable during the Holocene.

Changes in $\delta^{18}\text{O}_{sw}$ can be separated into two components: $\delta^{18}\text{O}$ change influenced by sea level change ($\delta^{18}\text{O}_{iv}$, global ice volume signal), and $\delta^{18}\text{O}$ change related to local hydrographic variation ($\delta^{18}\text{O}_{local}$). $\delta^{18}\text{O}_{local}$ can be calculated by subtracting $\delta^{18}\text{O}_{iv}$ from $\delta^{18}\text{O}_{sw}$ using the correction of $\delta^{18}\text{O}_{iv}$ reported by Waelbroeck et al. (2002). The results reveal that $\delta^{18}\text{O}_{local}$ was about 0.25‰ (VSMOW) between 17.3 and ~9.2 ka, and about 0.45‰ (VSMOW) after ~9.2 ka. Thus, local SSS in the southern OT was higher during the Holocene than during the last deglaciation (Fig. 4d).

Discussion

Factors influencing thermocline depth

The thermocline depth is controlled generally by wind stirring and convection (surface buoyancy flux) in the China seas. The surface buoyancy flux is the major factor influencing the

thermocline depth in the OT (Hao et al. 2012). The surface buoyancy flux consists of a thermal buoyancy flux, which is a function of net heat flux, and a haline buoyancy flux that is a function of precipitation and evaporation (Marshall and Schott 1999). The thermal buoyancy flux is one order of magnitude larger than the haline buoyancy flux in the OT (Hao et al. 2012). Therefore, the thermocline depth, or strength of upper water mixing, is influenced mainly by the surface thermal buoyancy or heat flux in the OT.

Changes in heat flux in the upper ocean result from an imbalance between input and output of heat through the sea surface. Major components of heat flux are insolation (inflow of solar energy), infrared radiation (heat loss by long-wave radiation), sensible heat flux (heat loss by conduction), latent heat flux (heat loss by evaporation), and advection (heat transfer by currents). Incoming solar energy tends to warm the sea surface and induce upper water stratification. As shown in Fig. 5a and b, the thermocline depth in the southern OT roughly corresponds to the annual mean insolation at 30°N (Berger and Loutre 1991). At ~14–8 ka, high insolation might have induced strong stratification, and thus the thermocline depth was shallow. Before and after this time period, insolation was low and stratification was weaker; hence, the thermocline depth increased at ~16.5–14.5 ka and ~7.5–4 ka.

Latent heat flux accounts for ~2/3 of the total heat loss (sum of infrared radiation, and sensible and latent heat fluxes) in the KC region (Chu et al. 2005). The evaporation causing latent heat loss is much higher in winter than in summer in the ECS (Chen et al. 1994; Chu et al. 2005), and is influenced primarily by wind speed and relative humidity. Therefore, the strong

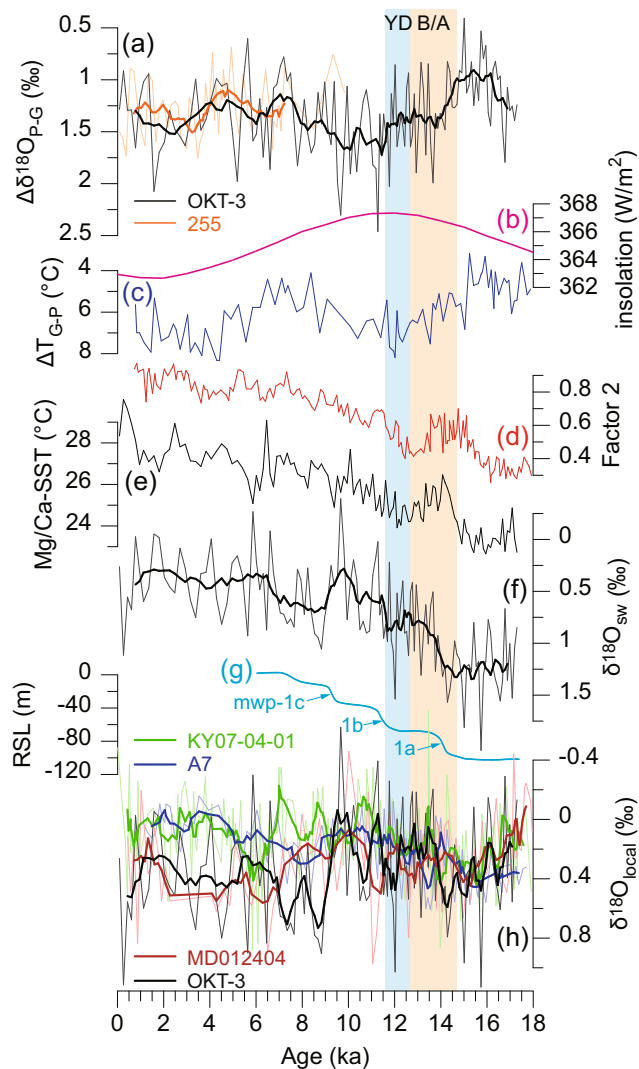


Fig. 5 Comparison of proxies. **a** $\Delta\delta^{18}\text{O}_{\text{P-G}}$ of this study and core 255 (Jian et al. 2000; bold lines 9-point running averages); **b** annual mean insolation at 30°N (Berger and Loutre 1991); **c** $\Delta T_{\text{G-P}}$, Mg/Ca -based temperature of *G. ruber* s.s. minus *P. obliquiloculata*, indicating the upper water thermal gradient in the northern South China Sea and the East Asian winter monsoon (Steinke et al. 2011); **d** Q-mode Factor 2 for core MD012404, indicating Kuroshio Current influence (Chang et al. 2008); **e** Mg/Ca -based sea surface temperature (SST) for core OKT-3 (Zhao et al. 2015); **f** $\delta^{18}\text{O}_{\text{sw}}$ of this study (bold line 9-point running average); **g** relative sea level (RSL) rise in the western Pacific (Liu et al. 2004; arrows melt water pulses, mwp); **h** $\delta^{18}\text{O}_{\text{local}}$ of this study, and for cores MD012404 (Chen et al. 2010), A7 (Sun et al. 2005) and KY07-04-1 (Kubota et al. 2010), bold lines 5-point running averages. YD Younger Dryas, B/A Bølling/Allerød

and dry East Asian winter monsoon (EAWM) plays a key role in heat loss in the KC region. As shown in Fig. 5a and c, the thermocline depth in the southern OT corresponds well to the EAWM proxy (Steinke et al. 2011). Strong EAWM induces intense surface heat (buoyancy) loss and upper water mixing, whereas weak EAWM favors stratification and shallow thermocline depth. A comparison can be made with the difference in Mg/Ca -based temperature between *G. ruber* and *P.*

obliquiloculata (Fig. 5c) indicating the thermocline depth in the northern South China Sea (SCS; Steinke et al. 2011). This suggests that changes in the upper water thermal structure in the southern OT and northern SCS are closely interconnected, probably by the EAWM.

The KC transports heat from low to high latitudes in the subtropical western North Pacific. Due to the KC influence, the latent and sensible heat fluxes are high (WHOI OAFflux Project), and thus the thermocline depth is deep in the KC region (Hao et al. 2012). Factor analysis of planktonic foraminifera has shown that KC influence has increased since the last deglaciation (Chang et al. 2008; Fig. 5d), which caused increasing SST in the southern OT (Zhao et al. 2015; Fig. 5e). Numerical experiments have demonstrated that KC volume transport was reduced when sea level was lower than that of the present day (Kao et al. 2006b; Lee et al. 2013). However, the thermocline depth trend does not correspond to the KC proxy (Fig. 5a, d) or KC volume transport trends. So, it appears that the influence of the KC on the thermocline depth is minor compared to that of the EAWM and insolation, despite the KC being a source of heat and promoting heat loss. This current influences surface, subsurface and intermediate waters in the OT (Oka and Kawabe 2003; Andres et al. 2008, 2015), but integrally warming the water column possibly has little effect on the thermal structure between the surface and subsurface layers.

Factors influencing sea surface salinity

The primary factor governing SSS is the global ice volume. Melting of ice sheets injects fresh water into the ocean, which not only reduces seawater salinity but also leads to eustatic sea level rise. As shown in Fig. 5f and g, long-term changes in the $\delta^{18}\text{O}_{\text{sw}}$ record of the southern OT and the relative sea level in the western Pacific (Liu et al. 2004) are well matched during the postglacial period. The lightening trend of the $\delta^{18}\text{O}_{\text{sw}}$ record is associated with a rise in sea level from 17.3 to ~ 9.2 ka. After ~ 9.2 ka the sea level was relatively stable, although it rose slightly at ~ 7.5 ka; likewise, $\delta^{18}\text{O}_{\text{sw}}$ remained relatively stable. Additionally, the melt water pulses 1a and 1b are associated with abrupt decreases in $\delta^{18}\text{O}_{\text{sw}}$ at ~ 14.2 and ~ 11.6 ka.

Lee et al. (2013) suggested that, during the last glacial period, there was little change in the KC path compared to that of the present day. By contrast, Kao et al. (2006b) proposed that the KC exited the OT through the Kerama Gap located southwest of the trough. Nevertheless, both studies agree with the existence of the KC in the southern OT. Therefore, the KC is another important factor controlling salinity in the southern OT since the last glaciation. KC influence and volume transport were weaker during the last deglaciation compared with the Holocene (Kao et al. 2006b; Chang et al. 2008; Lee et al. 2013). Indeed, local SSS was lower during the last deglaciation (Fig. 4d). Additionally, at ~ 9.2

ka when the melt water pulse 1c occurred, SSS did not decrease correspondingly but instead increased (Fig. 5f–h). This can plausibly be explained by an abrupt strengthening of the KC at ~ 9.4 ka (Xiang et al. 2007).

In the present study, variations in the $\Delta\delta^{18}\text{O}_{\text{P-G}}$, $\delta^{18}\text{O}_{\text{sw}}$, and $\delta^{18}\text{O}_{\text{local}}$ records are essentially synchronous at centennial to millennial timescales over the past 17,300 years. Thus, low (high) $\Delta\delta^{18}\text{O}_{\text{P-G}}$ values are mostly associated with high (low) $\delta^{18}\text{O}_{\text{sw}}$ and $\delta^{18}\text{O}_{\text{local}}$ values (Fig. 4). This aspect was assessed further by means of cross-correlation analyses, an approach successfully applied to non-stationary paleo-climate datasets (Marriner et al. 2012; Zheng et al. 2014). Negative coefficients of about -0.7 at Lag 0 values with confidence levels of 95% (Fig. 6) testify to the strong synchronicity between $\Delta\delta^{18}\text{O}_{\text{P-G}}$ and $\delta^{18}\text{O}_{\text{sw}}$ or $\delta^{18}\text{O}_{\text{local}}$. This means that SSS is high when upper water mixing is intense, and vice versa. According to modern oceanographic observations in the OT, salinity in the subsurface layer is usually higher than that in the surface layer due to the influence of the KC (Ichikawa and Beardsley 2002; Andres et al. 2008; Fig. 2e, f). If vertical mixing intensified, then saltier water at the top of the thermocline would be brought to the surface, causing an increase in SSS. Therefore, SSS is strongly influenced by upper water mixing at centennial to millennial timescales.

The CDW is the dominant source of fresh water in the ECS. Modern observations and simulations suggest that the CDW extends to the northeast toward the Tsushima Strait (Beardsley et al. 1985; Chang and Isobe 2003). Since ~ 9.2 ka, the sea

level and the Changjiang river mouth have been close to their modern positions (Liu et al. 2004, 2007), and intensified rainfall might have increased the fresh water flux (Dykoski et al. 2005; Jiang et al. 2007). Indeed, local SSS signatures differ strongly between cores OKT-3 (this study), MD012404 (Chen et al. 2010), A7 (Sun et al. 2005) and KY07-04-1 (Kubota et al. 2010), and salinity in the southern OT exceeded that of the northern OT after ~ 9.2 ka (Fig. 5h), implying that CDW influence was strong in the northern OT but weak in the southern OT. Differences in local SSS amongst these cores were small before ~ 9.2 ka (Fig. 5h), implying that the influence of fresh water was similar from the southern to northern OT. In view of the large dimensions of the trough (more than 1,000 km long), it is suggested that CDW influence was minimal in the OT before ~ 9.2 ka. In fact, Lee et al. (2013) proposed that, although there might have been an influence of fresh water on the continental shelf, the effect was minimal in the OT during the glacial period. Furthermore, precipitation and evaporation are two potential factors that inversely influence SSS. Today, their net effect is limited (annual precipitation largely counterbalances evaporation; Chen et al. 1994; Chu et al. 2005). However, it remains unclear whether or not this was the case in the past 17,300 years.

Millennial-scale climate changes

Previous studies suggested that variations in SST and planktonic foraminiferal abundance in the OT were nearly synchronous with abrupt millennial-scale climate changes in the North Atlantic, such as the B/A and YD events (Ijiri et al. 2005; Sun et al. 2005; Xiang et al. 2007; Yu et al. 2009; Kubota et al. 2010; Ruan et al. 2015). However, an Antarctic-like signal was found in core MD012404 (Chen et al. 2010), and the SST of core OKT-3 also corresponds to the timing of the Antarctic Cold Reversal during the B/A event (Zhao et al. 2015). The $\delta^{18}\text{O}$ record of core OKT-3 argues against those SST records. The SSSs of core OKT-3 and other cores in the OT show no anomalous changes during the B/A and YD events (Sun et al. 2005; Chen et al. 2010; Kubota et al. 2010; Fig. 5f, h). This can be ascribed to interaction between the KC and precipitation. During the YD period, for example, weak monsoonal rainfall (Dykoski et al. 2005) tended to increase SSS, but a weak KC (Chang et al. 2008) tended to decrease SSS. Chen et al. (2010) also found that the KC might have played a more dynamic role than commonly considered, competing with atmospheric teleconnection with the high-latitude North Atlantic. Additionally, the *Pulleniatina* Minimum Event, widely recorded in the western North Pacific between 4.5 and 3 ka, is not distinguished in the $\delta^{18}\text{O}_{\text{local}}$ and $\Delta\delta^{18}\text{O}_{\text{P-G}}$ records of core OKT-3 (Figs. 4 and 5). Similarly, Lin et al. (2006) reported no distinctive anomalies in paleoceanographic proxies for this event.

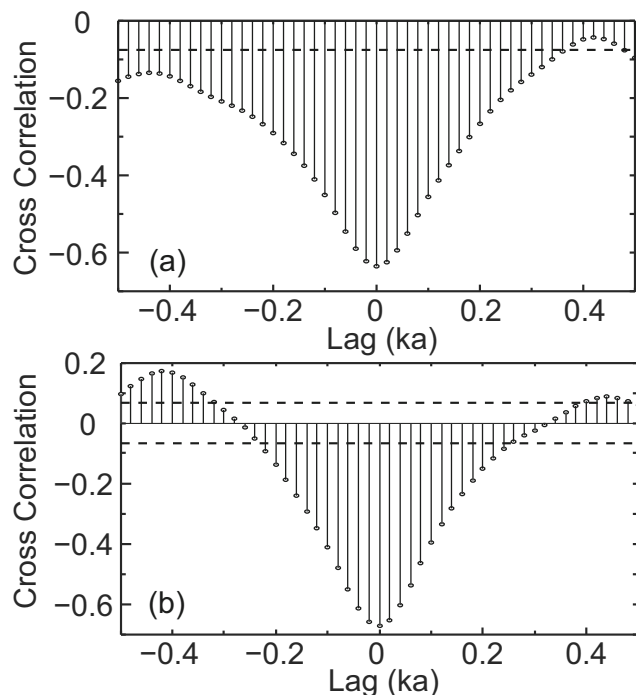


Fig. 6 Cross-correlation analyses **a** between $\Delta\delta^{18}\text{O}_{\text{P-G}}$ and $\delta^{18}\text{O}_{\text{sw}}$, and **b** between $\Delta\delta^{18}\text{O}_{\text{P-G}}$ and $\delta^{18}\text{O}_{\text{local}}$. Dash lines 95% confidence bounds

Possible teleconnection between the OT and global climate change was assessed by means of wavelet and spectral analyses of the $\Delta\delta^{18}\text{O}_{\text{P-G}}$ and $\delta^{18}\text{O}_{\text{local}}$ time series. For the wavelet analysis, the time series were resampled at 20 year resolution, and methods reported by Torrence and Compo (1998) and Grinsted et al. (2004) were used. The spectral analysis employed the REDFIT software of Schulz and Mudelsee (2002). The findings reveal 1,540-, 860- and 640-year periods for $\Delta\delta^{18}\text{O}_{\text{P-G}}$ (Fig. 7a, b), and 1,480-, 1,050- and 630-year periods for $\delta^{18}\text{O}_{\text{local}}$ (Fig. 7c, d).

As discussed above, the thermocline depth is influenced mainly by insolation and the EAWM, and the local SSS is influenced mainly by the KC and vertical mixing (thermocline depth). The 1,540- and 1,480-year periods of the $\Delta\delta^{18}\text{O}_{\text{P-G}}$ and $\delta^{18}\text{O}_{\text{local}}$ time series agree with the pervasive 1,500-year period in global climate records. This period originates from internal response of the THC to external solar forcing (Dima and Lohmann 2009). The EAWM and KC also display a periodicity of 1,500 years (Garidel-Thoron et al. 2001; Isono et al. 2009). Soon et al. (2014) identified a fundamental solar periodicity of 1,000 years and an intermediary derived cycle of 700 years that might mark rectified responses of the THC to external solar modulation. The 1,050-year periodicity of the present study agrees with the fundamental solar periodicity of 1,000 years; the 860-, 640- and 630-year periods can be ascribed to the intermediary derived solar cycle of 700 years.

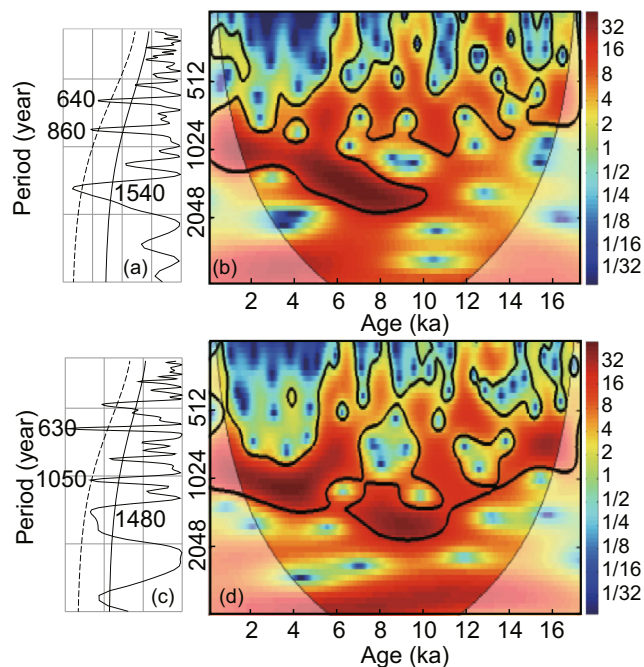


Fig. 7 a Spectral and b wavelet analyses of $\Delta\delta^{18}\text{O}_{\text{P-G}}$. c, d Corresponding data for $\delta^{18}\text{O}_{\text{local}}$

Conclusions

Oxygen isotope analyses of the planktonic foraminifers *G. ruber* s.s. and *P. obliquiloculata* from the AMS ^{14}C dated OKT-3 core spanning the past 17,300 years in the southern Okinawa Trough revealed that the thermocline depth ($\Delta\delta^{18}\text{O}_{\text{P-G}}$) was influenced mainly by the surface thermal buoyancy flux or air–sea heat flux, which varied with annual mean insolation and the East Asian winter monsoon. Changes in thermocline depth in the southern OT (East China Sea) and northern South China Sea are interconnected. SSS ($\delta^{18}\text{O}_{\text{sw}}$) was influenced primarily by global ice volume and the Kuroshio Current. Vertical mixing is another important factor controlling SSS on centennial to millennial timescales. After ~ 9.2 ka, differences in local SSS ($\delta^{18}\text{O}_{\text{local}}$) amongst several cores spanning the northern to southern OT became more pronounced, and salinity in the north was lower than in the south, indicating a stronger influence of Changjiang diluted water in the northern sector. KC activity probably disturbed the atmospheric teleconnection with the North Atlantic, so that anomalous changes in SSS are not obvious in abrupt millennial-scale climate events such as the B/A and YD. Wavelet and spectral analyses of the $\Delta\delta^{18}\text{O}_{\text{P-G}}$ and $\delta^{18}\text{O}_{\text{local}}$ records show 1,540-, 1,480-, 1,050-, 860-, 640-, and 630-year periods involving solar, EAWM and KC signals over the last 17,300 years in the southern Okinawa Trough.

Acknowledgements This work was financially supported by the National Natural Science Foundation of China (grant numbers 41406074, 41476052 and 40906033), the Open Foundation of the Key Laboratory of Marine Hydrocarbon Resources and Environmental Geology (grant number MRE201405) and the China Geological Survey Project (grant number GZH201500203). We thank two reviewers and the journal editors for their constructive comments.

Conflict of interest The authors declare that there is no conflict of interest with third parties.

References

- Andres M, Wimbush M, Park JH, Chang KI, Lim BH, Watts DR, Ichikawa H, Teague WJ (2008) Observations of Kuroshio flow variations in the East China Sea. *J Geophys Res* 113, C05013. doi:10.1029/2007JC004200
- Andres M, Jan S, Sanford T, Mensah V, Centurioni L, Book J (2015) Mean structure and variability of the Kuroshio from northeastern Taiwan to southwestern Japan. *Oceanography* 28:84–95. doi:10.5670/oceanog.2015.84
- Beardsley R, Limeburner R, Yu H, Cannon G (1985) Discharge of the Changjiang (Yangtze river) into the East China sea. *Cont Shelf Res* 4:57–76
- Bemis BE, Spero HJ, Bijma J, Lea DW (1998) Reevaluation of the oxygen isotopic composition of planktonic foraminifera: experimental results and revised paleotemperature equations. *Paleoceanography* 13:150–160. doi:10.1029/98PA00070

- Berger A, Loutre MF (1991) Insolation values for the climate of the last 10 million years. *Quat Sci Rev* 10:297–317. doi:10.1016/0277-3791(91)90033-Q
- Bond G, Broecker W, Johnsen S, McManus J, Labeyrie L, Jouzel J, Bonani G (1993) Correlations between climate records from North Atlantic sediments and Greenland ice. *Nature* 365:143–147
- Bond G, Showers W, Cheseby M, Lotti R, Almasi P, Priore P, Cullen H, Hajdas I, Bonani G (1997) A pervasive millennial-scale cycle in North Atlantic Holocene and glacial climates. *Science* 278:1257–1266
- Bond G, Kromer B, Beer J, Muscheler R, Evans MN, Showers W, Hoffmann S, Lotti-Bond R, Hajdas I, Bonani G (2001) Persistent solar influence on North Atlantic climate during the Holocene. *Science* 294:2130–2136
- Chang P-H, Isobe A (2003) A numerical study on the Changjiang diluted water in the Yellow and East China Seas. *J Geophys Res* 108:3299. doi:10.1029/2002JC001749
- Chang Y-P, Wang W-L, Yokoyama Y, Matsuzaki H, Kawahata H, Chen M-T (2008) Millennial-scale planktic foraminifer faunal variability in the East China Sea during the past 40000 years (IMAGES MD12404 from the Okinawa Trough). *Terr Atmos Ocean Sci* 19: 389–401
- Chang Y-P, Chen M-T, Yokoyama Y, Matsuzaki H, Thompson WG, Kao S-J, Kawahata H (2009) Monsoon hydrography and productivity changes in the East China Sea during the past 100,000 years: Okinawa Trough evidence (MD012404). *Paleoceanography* 24, PA3208. doi:10.1029/2007PA001577
- Chen C, Beardsley RC, Limeburner R, Kim K (1994) Comparison of winter and summer hydrographic observations in the Yellow and East China Seas and adjacent Kuroshio during 1986. *Cont Shelf Res* 14:909–929. doi:10.1016/0278-4343(94)90079-5
- Chen MT, Lin XP, Chang YP, Chen YC, Lo L, Shen CC, Yokoyama Y, Oppo DW, Thompson WG, Zhang R (2010) Dynamic millennial-scale climate changes in the northwestern Pacific over the past 40,000 years. *Geophys Res Lett* 37, L23603. doi:10.1029/2010GL045202
- Chu P, Yuchun C, Kuninaka A (2005) Seasonal variability of the Yellow Sea/East China Sea surface fluxes and thermohaline structure. *Adv Atmos Sci* 22:1–20. doi:10.1007/BF02930865
- Dansgaard W, Johnsen SJ, Clausen HB, Dahl-Jensen D, Gundestrup NS, Hammer CU, Hvidberg CS, Steffensen JP, Sveinbjornsdottir AE, Jouzel J, Bond G (1993) Evidence for general instability of past climate from a 250-kyr ice-core record. *Nature* 364:218–220
- Dima M, Lohmann G (2009) Conceptual model for millennial climate variability: a possible combined solar-thermohaline circulation origin for the ~1,500-year cycle. *Clim Dyn* 32:301–311. doi:10.1007/s00382-008-0471-x
- Dykoski CA, Edwards RL, Cheng H, Yuan D, Cai Y, Zhang M, Lin Y, Qing J, An Z, Revenaugh J (2005) A high-resolution, absolute-dated Holocene and deglacial Asian monsoon record from Dongge Cave, China. *Earth Planet Sci Lett* 233:71–86. doi:10.1016/j.epsl.2005.01.036
- Garidel-Thoron T, Beaufort L, Linsley BK, Dannenmann S (2001) Millennial-scale dynamics of the East Asian winter monsoon during the last 200,000 years. *Paleoceanography* 16:491–502
- Grinsted A, Moore JC, Jevrejeva S (2004) Application of the cross wavelet transform and wavelet coherence to geophysical time series. *Nonlinear Process Geophys* 11:561–566. doi:10.5194/npg-11-561-2004
- Grootes PM, Stuiver M, White JWC, Johnsen S, Jouzel J (1993) Comparison of oxygen isotope records from the GISP2 and GRIP Greenland ice cores. *Nature* 366:552–554
- Hao J, Chen Y, Wang F, Lin P (2012) Seasonal thermocline in the China Seas and northwestern Pacific Ocean. *J Geophys Res* 117, C02022. doi:10.1029/2011JC007246
- Ichikawa H, Beardsley R (2002) The current system in the Yellow and East China Seas. *J Oceanogr* 58:77–92. doi:10.1023/A:1015876701363
- Ijiri A, Wang L, Oba T, Kawahata H, Huang C-Y, Huang C-Y (2005) Paleoenvironmental changes in the northern area of the East China Sea during the past 42,000 years. *Palaeogeogr Palaeoclimatol Palaeoecol* 219:239–261. doi:10.1016/j.palaeo.2004.12.028
- Isono D, Yamamoto M, Irino T, Oba T, Murayama M, Nakamura T, Kawahata H (2009) The 1500-year climate oscillation in the midlatitude North Pacific during the Holocene. *Geology* 37:591–594. doi:10.1130/G25667A.1
- Jian Z, Wang P, Saito Y, Wang J, Pflaumann U, Oba T, Cheng X (2000) Holocene variability of the Kuroshio Current in the Okinawa Trough, northwestern Pacific Ocean. *Earth Planet Sci Lett* 184: 305–319. doi:10.1016/S0012-821X(00)00321-6
- Jiang T, Su B, Hartmann H (2007) Temporal and spatial trends of precipitation and river flow in the Yangtze River Basin, 1961–2000. *Geomorphology* 85:143–154. doi:10.1016/j.geomorph.2006.03.015
- Kagimoto T, Yamagata T (1997) Seasonal transport variations of the Kuroshio: an OGCM simulation. *J Phys Oceanogr* 27:403–418. doi:10.1175/1520-0485(1997)027<0403:STVOTK>2.0.CO;2
- Kao SJ, Horng CS, Hsu SC, Wei KY, Chen J, Lin YS (2005) Enhanced deepwater circulation and shift of sedimentary organic matter oxidation pathway in the Okinawa Trough since the Holocene. *Geophys Res Lett* 32, L15609. doi:10.1029/2005GL023139
- Kao SJ, Roberts AP, Hsu SC, Chang YP, Lyons WB, Chen MT (2006a) Monsoon forcing, hydrodynamics of the Kuroshio Current, and tectonic effects on sedimentary carbon and sulfur cycling in the Okinawa Trough since 90 ka. *Geophys Res Lett* 33, L05610. doi:10.1029/2005GL025154
- Kao SJ, Wu C-R, Hsin Y-C, Dai M (2006b) Effects of sea level change on the upstream Kuroshio Current through the Okinawa Trough. *Geophys Res Lett* 33, L16604. doi:10.1029/2006GL026822
- Kao SJ, Dai MH, Wei KY, Blair NE, Lyons WB (2008) Enhanced supply of fossil organic carbon to the Okinawa Trough since the last deglaciation. *Paleoceanography* 23, PA2207. doi:10.1029/2007PA001440
- Kubota Y, Kimoto K, Tada R, Oda H, Yokoyama Y, Matsuzaki H (2010) Variations of East Asian summer monsoon since the last deglaciation based on Mg/Ca and oxygen isotope of planktic foraminifera in the northern East China Sea. *Paleoceanography* 25, PA4205. doi:10.1029/2009PA001891
- Lee KE, Lee HJ, Park J-H, Chang Y-P, Ikehara K, Itaki T, Kwon HK (2013) Stability of the Kuroshio path with respect to glacial sea level lowering. *Geophys Res Lett* 40:392–396. doi:10.1012/grl.50102
- LeGrande AN, Schmidt GA (2011) Water isotopologues as a quantitative paleosalinity proxy. *Paleoceanography* 26, PA3225. doi:10.1029/2010PA002043
- Lin Y-S, Wei K-Y, Lin I-T, Yu P-S, Chiang H-W, Chen C-Y, Shen C-C, Mii H-S, Chen Y-G (2006) The Holocene *Pulleniatina* Minimum Event revisited: geochemical and faunal evidence from the Okinawa Trough and upper reaches of the Kuroshio current. *Mar Micropaleontol* 59:153–170. doi:10.1016/j.marmicro.2006.02.003
- Liu Z, Gan J (2012) Variability of the Kuroshio in the East China Sea derived from satellite altimetry data. *Deep-Sea Res I* 59:25–36. doi:10.1016/j.dsr.2011.10.008
- Liu JP, Milliman JD, Gao S, Cheng P (2004) Holocene development of the Yellow River's subaqueous delta, North Yellow Sea. *Mar Geol* 209:45–67. doi:10.1016/j.margeo.2004.06.009
- Liu JP, Xu KH, Li AC, Milliman JD, Velozzi DM, Xiao SB, Yang ZS (2007) Flux and fate of Yangtze River sediment delivered to the East China Sea. *Geomorphology* 85:208–224. doi:10.1016/j.geomorph.2006.03.023
- Locarnini RA, Mishonov AV, Antonov JI and 9 others (2013) World Ocean Atlas 2013, Volume 1: Temperature. In: Levitus S, Mishonov A (eds) NOAA Atlas NESDIS 73, 40 pp

- Marriner N, Flaux C, Kaniewski D, Morhange C, Leduc G, Moron V, Chen Z, Gasse F, Empereur J-Y, Stanley J-D (2012) ITCZ and ENSO-like pacing of Nile delta hydro-geomorphology during the Holocene. *Quat Sci Rev* 45:73–84. doi:10.1016/j.quascirev.2012.04.022
- Marshall J, Schott F (1999) Open-ocean convection: observations, theory, and models. *Rev Geophys* 37:1–64
- Oka E, Kawabe M (2003) Dynamic structure of the Kuroshio south of Kyushu in relation to the Kuroshio path variations. *J Oceanogr* 59: 595–608. doi:10.1023/B:JOCE.0000009589.28241.93
- Pflaumann U, Jian Z (1999) Modern distribution patterns of planktonic foraminifera in the South China Sea and western Pacific: a new transfer technique to estimate regional sea-surface temperatures. *Mar Geol* 156:41–83. doi:10.1016/S0025-3227(98)00173-X
- Qu T, Lukas R (2003) The bifurcation of the North Equatorial Current in the Pacific. *J Phys Oceanogr* 33:5–18. doi:10.1175/1520-0485(2003)033<0005:TBOTNE>2.0.CO;2
- Ravelo AC, Fairbanks RG (1992) Oxygen isotopic composition of multiple species of planktonic foraminifera: recorders of the modern photic zone temperature gradient. *Paleoceanography* 7:815–831. doi:10.1029/92PA02092
- Reimer PJ, Bard E, Bayliss A et al (2013) IntCal13 and Marine13 radiocarbon age calibration curves 0–50,000 years cal BP. *Radiocarbon* 55:1869–1887. doi:10.2458/azu_js_rc.55.16947
- Ruan J, Xu Y, Ding S, Wang Y, Zhang X (2015) A high resolution record of sea surface temperature in southern Okinawa Trough for the past 15,000 years. *Palaeogeogr Palaeoclimatol Palaeoecol* 426:209–215. doi:10.1016/j.palaeo.2015.03.007
- Schulz M, Mudelsee M (2002) REDFIT: estimating red-noise spectra directly from unevenly spaced paleoclimatic time series. *Comput Geosci* 28:421–426. doi:10.1016/S0098-3004(01)00044-9
- Sirocko F, Garbe-Schönberg D, McIntyre A, Molfino B (1996) Teleconnections between the subtropical monsoons and high-latitude climates during the last deglaciation. *Science* 272:526–529
- Soon W, Velasco Herrera VM, Selvaraj K et al (2014) A review of Holocene solar-linked climatic variation on centennial to millennial timescales: physical processes, interpretative frameworks and a new multiple cross-wavelet transform algorithm. *Earth-Sci Rev* 134:1–15. doi:10.1016/j.earscirev.2014.03.003
- Steinke S, Glatz C, Mohtadi M, Groenewald J, Li Q, Jian Z (2011) Past dynamics of the East Asian monsoon: no inverse behaviour between the summer and winter monsoon during the Holocene. *Global Planet Change* 78:170–177. doi:10.1016/j.gloplacha.2011.06.006
- Stuiver M, Reimer PJ (1993) Extended ^{14}C data base and revised CALIB 3.0 ^{14}C age calibration program. *Radiocarbon* 35:215–230
- Sun Y, Oppo DW, Xiang R, Liu W, Gao S (2005) Last deglaciation in the Okinawa Trough: subtropical northwest Pacific link to Northern Hemisphere and tropical climate. *Paleoceanography* 20, PA4005. doi:10.1029/2004PA001061
- Tian J, Wang P, Chen R, Cheng X (2005) Quaternary upper ocean thermal gradient variations in the South China Sea: implications for east Asian monsoon climate. *Paleoceanography* 20, PA4007. doi:10.1029/2004PA001115
- Torrence C, Compo GP (1998) A practical guide to wavelet analysis. *Bull Am Meteorol Soc* 79:61–78. doi:10.1175/1520-0477(1998)079<0061:APGTWA>2.0.CO;2
- Ujiié H, Ujiié Y (1999) Late Quaternary course changes of the Kuroshio Current in the Ryukyu Arc region, northwestern Pacific Ocean. *Mar Micropaleontol* 37:23–40. doi:10.1016/S0377-8398(99)00010-9
- Ujiié Y, Ujiié H, Taira A, Nakamura T, Oguri K (2003) Spatial and temporal variability of surface water in the Kuroshio source region, Pacific Ocean, over the past 21,000 years: evidence from planktonic foraminifera. *Mar Micropaleontol* 49:335–364. doi:10.1016/S0377-8398(03)00062-8
- Waelbroeck C, Labeyrie L, Michel E, Duplessy JC, McManus JF, Lambeck K, Balbon E, Labracherie M (2002) Sea-level and deep water temperature changes derived from benthic foraminifera isotopic records. *Quat Sci Rev* 21:295–305. doi:10.1016/S0277-3791(01)00101-9
- Wang L (2000) Isotopic signals in two morphotypes of *Globigerinoides ruber* (white) from the South China Sea: implications for monsoon climate change during the last glacial cycle. *Palaeogeogr Palaeoclimatol Palaeoecol* 161:381–394. doi:10.1016/S0031-0182(00)00094-8
- Wang Y, Cheng H, Edwards RL, He Y, Kong X, An Z, Wu J, Kelly MJ, Dykoski CA, Li X (2005) The Holocene Asian monsoon: links to solar changes and North Atlantic climate. *Science* 308:854–857. doi:10.1126/science.1106296
- Wu L, Li C, Yang C, Xie S-P (2008) Global teleconnections in response to a shutdown of the Atlantic meridional overturning circulation. *J Clim* 21:3002–3019. doi:10.1175/2007JCLI1858.1
- Xiang R, Sun Y, Li T, Oppo DW, Chen M, Zheng F (2007) Paleoenvironmental change in the middle Okinawa Trough since the last deglaciation: evidence from the sedimentation rate and planktonic foraminiferal record. *Palaeogeogr Palaeoclimatol Palaeoecol* 243:378–393. doi:10.1016/j.palaeo.2006.08.016
- Xu X, Oda M (1999) Surface-water evolution of the eastern East China Sea during the last 36,000 years. *Mar Geol* 156:285–304. doi:10.1016/S0025-3227(98)00183-2
- Xu X, Yamasaki M, Oda M, Honda MC (2005) Comparison of seasonal flux variations of planktonic foraminifera in sediment traps on both sides of the Ryukyu Islands, Japan. *Mar Micropaleontol* 58:45–55. doi:10.1016/j.marmicro.2005.09.002
- Xu D, Lu H, Wu N, Liu Z, Li T, Shen C, Wang L (2013) Asynchronous marine-terrestrial signals of the last deglacial warming in East Asia associated with low- and high-latitude climate changes. *Proc Natl Acad Sci U S A* 110:9657–9662. doi:10.1073/pnas.1300025110
- Yamamoto M, Kishizaki M, Oba T, Kawahata H (2013) Intense winter cooling of the surface water in the northern Okinawa Trough during the last glacial period. *J Asian Earth Sci* 69:86–92. doi:10.1016/j.jseaes.2012.06.011
- Yamasaki M, Oda M (2003) Sedimentation of planktonic foraminifera in the East China Sea: evidence from a sediment trap experiment. *Mar Micropaleontol* 49:3–20. doi:10.1016/S0377-8398(03)00024-0
- Yonedo M, Uno H, Shibata Y, Suzuki R, Kumamoto Y, Yoshida K, Sasaki T, Suzuki A, Kawahata H (2007) Radiocarbon marine reservoir ages in the western Pacific estimated by pre-bomb molluscan shells. *Nucl Instrum Methods Phys Res B* 259: 432–437. doi:10.1016/j.nimb.2007.01.184
- Yu H, Liu Z, Berné S, Jia G, Xiong Y, Dickens GR, Wei G, Shi X, Liu JP, Chen F (2009) Variations in temperature and salinity of the surface water above the middle Okinawa Trough during the past 37 kyr. *Palaeogeogr Palaeoclimatol Palaeoecol* 281:154–164. doi:10.1016/j.palaeo.2009.08.002
- Zhang J, Yu H, Jia G, Chen F, Liu Z (2010) Terrestrial *n*-alkane signatures in the middle Okinawa Trough during the post-glacial transgression: control by sea level and paleovegetation confounded by offshore transport. *Geo-Mar Lett* 30:143–150. doi:10.1007/s00367-009-0173-3
- Zhao M, Huang C-Y, Wei K-Y (2005) A 28,000 year U_{37}^{K} sea-surface temperature record of ODP Site 1202B, the southern Okinawa Trough. *Terr Atmos Ocean Sci* 16:45–56
- Zhao J, Li J, Cai F, Wei H, Hu B, Dou Y, Wang L, Xiang R, Cheng H, Dong L, Zhang CL (2015) Sea surface temperature variation during the last deglaciation in the southern Okinawa Trough: modulation of high latitude teleconnections and the Kuroshio Current. *Prog Oceanogr* 138:238–248. doi:10.1016/j.pocean.2015.06.008

- Zheng X, Li A, Wan S, Jiang F, Kao SJ, Johnson C (2014) ITCZ and ENSO pacing on East Asian winter monsoon variation during the Holocene: sedimentological evidence from the Okinawa Trough. *J Geophys Res* 119:4410–4429. doi:[10.1002/2013JC009603](https://doi.org/10.1002/2013JC009603)
- Zhou H, Li T, Jia G, Zhu Z, Chi B, Cao Q, Sun R, Pa P (2007) Sea surface temperature reconstruction for the middle Okinawa Trough during the last glacial–interglacial cycle using C_{37} unsaturated alkenones. *Palaeogeogr Palaeoclimatol Palaeoecol* 246:440–453. doi:[10.1016/j.palaeo.2006.10.011](https://doi.org/10.1016/j.palaeo.2006.10.011)
- Zweng MM, Reagan JR, Antonov JI, Locarnini RA, Mishonov AV, Boyer TP, Garcia HE, Baranova OK, Johnson DR, Seidov D, Biddle MM (2013) World Ocean Atlas 2013, Volume 2: Salinity. In: Levitus S, Mishonov A (eds) NOAA Atlas NESDIS 74, 39 pp